

## Computational models and tools for developing sophisticated stimulation strategies for retinal neuroprostheses

**Author:**

Guo, T; Tsai; Muralidharan; Suaning; Morley; Dokos; Lovell

**Publication details:**

Proceedings of the Annual International Conference of the IEEE Engineering in Medicine and Biology Society, EMBS

v. 2018-July

Medium: Print

pp. 2248 - 2251

9781538636466 (ISBN)

1557-170X (ISSN); 1558-4615 (ISSN)

**Event details:**

Engineering in Medicine and Biology Society (EMBC), 2018 Annual International Conference of the IEEE.

Honolulu, US

2018-07-18 - 2018-07-22

**Publication Date:**

2018-07-18

**Publisher DOI:**

<https://doi.org/10.1109/embc.2018.8512748>

**License:**

<https://creativecommons.org/licenses/by-nc-nd/4.0/>

Link to license to see what you are allowed to do with this resource.

Downloaded from [http://hdl.handle.net/1959.4/unsworks\\_60925](http://hdl.handle.net/1959.4/unsworks_60925) in <https://unsworks.unsw.edu.au> on 2024-04-26

# Computational models and tools for developing sophisticated stimulation strategies for retinal neuroprostheses

Tianruo Guo, *Member, IEEE*, David Tsai, *Member, IEEE*, Madhuvanthy Muralidharan, *Student Member, IEEE*, Mingli Li, *Member, IEEE*, Gregg J. Suaning, *Senior Member, IEEE*, John W. Morley, Socrates Dokos, *Member, IEEE*, Nigel H. Lovell, *Fellow, IEEE*

**Abstract**— Improvements to the efficacy of retinal neuroprostheses can be achieved by developing more sophisticated neural stimulation strategies to enable selective or preferential activation of specific retinal ganglion cells (RGCs). Computational models are particularly well suited for these investigations. The electric field can be accurately described by mathematical formalisms, and the population-based neural responses to the electrical stimulation can be investigated at resolutions well beyond those achievable by current state-of-the-art biological techniques.

In this study, we used a biophysically- and morphologically-detailed RGC model to explore the ability of high frequency electrical stimulation (HFS) to preferentially activate ON and OFF RGC subtypes, the two major information pathways of the retina. The performance of a wide range of electrical stimulation amplitudes (0 - 100  $\mu\text{A}$ ) and frequencies (1 - 10 kHz) on functionally-distinct RGC responses were evaluated. We found that ON RGCs could be preferentially activated at relatively higher stimulation amplitudes ( $> 50 \mu\text{A}$ ) and frequencies ( $> 2 \text{ kHz}$ ) while OFF RGCs were activated by lower stimulation amplitudes (10 to 50  $\mu\text{A}$ ) across all tested frequencies. These stimuli also show great promise in eliciting RGC responses that parallel RGC encoding: one RGC type exhibited an increase in spiking activity during electrical stimulation whilst another exhibited decreased spiking activity, given the same stimulation parameters.

## I. INTRODUCTION

Retinitis pigmentosa leads to progressive loss of photoreceptors, resulting in profound vision impairment. Retinal neuroprostheses aim to restore patterned vision to those with vision loss by electrically stimulating the remaining neurons in the degenerate retina. Over the past few decades, research into retinal neuroprostheses has shown several encouraging achievements, including the ability to elicit visual percepts or phosphenes in human patients. These studies however, also reported limited visual acuity (20/1262 for the Argus II and 20/546 for Alpha-IMS) - values far lower than what is considered to be legally blind (20/200).

This research was supported by the National Health and Medical Research Council (NHMRC, Project Grants RG1087224 and RG1063046).

T. Guo, D. Tsai, M. Muralidharan, G. J. Suaning, S. Dokos and N. H. Lovell are with the Graduate School of Biomedical Engineering, UNSW, Sydney, Australia. D. Tsai is also with Biological Sciences and Electrical Engineering, Columbia University, New York, USA. J. W. Morley is with the School of Medicine, Western Sydney University, Australia. L. Li is with School of Biomedical Engineering, SJTU, Shanghai, China.

E-mail for correspondence: n.lovell@unsw.edu.au

Moreover, the phosphenes evoked by all implants tested to date have remained complex, with human subjects reporting evoked percepts that resembled halos, blobs, wedges, streaks, or other shapes [1-4]. A primary reason for the inability of existing retinal neuroprostheses to provide higher visual resolution and better visual perception could be the indiscriminate activation of different neuronal types across large regions of the retina, providing conflicting information to higher visual centers. To address this problem, we require an improved understanding of how different functional retinal ganglion cell (RGC) types respond to artificial electrical stimulation. In particular, if different RGC types can be selectively or preferentially activated in a desired temporospatial sequence, the elicited signals may be interpreted and translated more accurately by the brain, giving rise to visual percepts of greater meaning and utility.

Previous reports have indicated that 2-kHz high frequency electrical stimulation (HFS) may elicit preferential excitation of different RGCs in a manner similar to RGC responses to light stimuli in a healthy retina [5-8]. To test whether a larger range of HFS parameters can improve or even maximize the preferential excitation of ON and OFF RGC pathways, we conducted *in silico* investigations using biophysically- and morphologically-detailed computational models of ON and OFF RGCs in the NEURON computational environment, to evaluate the performance of a range of electrical stimulation amplitudes (10 - 100  $\mu\text{A}$ ) and frequencies (1 - 10 kHz) on RGC responses. In addition, in order to investigate the effect of ON and OFF RGC dendritic morphologies on HFS-induced responses, we developed a neural morphology generator, capable of generating RGCs with tunable morphological properties, including the dendritic field radius, total dendritic length and stratification level [9].

## II. METHODOLOGY

### A. Computational Model of ON and OFF RGC Clusters

ON and OFF RGC clusters were implemented using the NEURON computational software [10]. The techniques we used for modelling individual RGCs have been described in detail previously [11, 12]. We employed a custom neural morphology generator, adapted from an existing neuronal morphology generation approach [12, 13], to simulate the different dendritic morphological structures of ON and OFF RGCs (see Fig. 1A). The RGC soma was initially defined as a point at the origin. With the soma as the center, a number of random carrier points, which serve as the basis of dendritic

growth, were distributed within a circular planar region having a user-defined radius. An algorithm, based on the minimum spanning tree algorithm [14], generated dendritic branches by connecting unconnected carrier points to nodal points of the tree. After creating the dendritic tree, the soma was then extended into a 15  $\mu\text{m}$  segment. A 50  $\mu\text{m}$  long axonal hillock and a 1000  $\mu\text{m}$  long axon were added subsequently. The vertical distance between the axon and the soma was set to 10  $\mu\text{m}$ , and the first 50  $\mu\text{m}$  segment of the axon was defined as the axonal initial segment (AIS).

RGC dendritic morphological parameters [9], including dendritic field radius ( $\mu\text{m}$ ), total dendritic length ( $\mu\text{m}$ ) and stratification level ( $\mu\text{m}$ ), were adjusted based on published statistics of RGC morphologies (see Table I). ON and OFF RGC models shared the kinetic-defining parameters of all ionic currents. The ionic channel distributions were compartment-specific, to reflect the proportion of channels in specific regions of each RGC. The estimated maximum membrane conductance values ( $\text{mS}/\text{cm}^2$ ) per region in each cell are listed in Table II.

### B. Extracellular Electrical Stimulation

To simulate extracellular stimulation, an analytic formulation of the extracellular potential at each spatial point was adapted based on previous studies [15-17]. The extracellular domain was considered to be homogeneous, and extracellular resistivity was set to 500  $\Omega\cdot\text{cm}$  [16]. Cathodic-first, charge-balanced, symmetric, constant-current biphasic stimuli, each with a pulse width of 50  $\mu\text{s}$  per phase, were used without an inter-phase interval. The extracellular stimulus amplitude ranged from 10 to 100  $\mu\text{A}$  in 5  $\mu\text{A}$  steps, and stimulus frequencies ranged from 1.0 to 10 kHz in 0.5 kHz steps. All pulse trains were 200 ms in duration.

For each RGC model, we defined a 3D Cartesian ( $x, y, z$ ) coordinate system, with the soma as the origin, such that the upper surface of the RGC dendritic field was aligned in the  $x$ - $y$  plane and the RGC axon was aligned with the  $y$ -axis. A hexapolar electrode array (each disc electrode of 15  $\mu\text{m}$  radius, with center-to-center distance of 60  $\mu\text{m}$ ) was positioned at location (0, -40, -50)  $\mu\text{m}$ , where (0, 0, 0)  $\mu\text{m}$  are the local 3D coordinates of the soma (see Fig. 1A).

## III. RESULTS

Fig. 1B1 illustrates the stimulus-dependent (from 10 to 100  $\mu\text{A}$ ) ON and OFF RGC action potential spike counts (spikes/200 ms) in response to a large range of stimulation frequencies (from 1 to 10 kHz). The elicited spikes were observed and counted at the soma. Our model predicted that the elicited RGC spike counts are highly dependent on stimulating frequency and amplitude. The colors in Fig 1B1 denote the number of evoked spikes for a given stimulation frequency and pulse amplitude from ON or OFF cells. The total spike count (spikes/200 ms) of the ON cell reached a plateau as the stimulus current increased above a certain threshold at frequencies up to 5.5 kHz. However, with frequencies higher than 6 kHz, the total spike number (spikes/200 ms) increased initially with stimulus amplitude, followed by a decline with further amplitude increase,

creating a non-monotonic surface in the frequency-amplitude topological space. In contrast, the OFF cell exhibited a non-monotonic profile at stimulation frequencies higher than 1.5 kHz. With increasing stimulation frequency, both ON and OFF RGCs exhibited an increased slope of the rising phase in spikes/ $\mu\text{A}$  (the epoch in which spike counts increase with increasing stimulation current) and concomitantly, an earlier onset of the falling phase (in which the total spike numbers saturated or declined). Finally, both activation maps indicated a decreasing stimulation threshold trend to HFS pulse trains with increasing stimulation frequency, where threshold was defined as the stimulation amplitude capable of eliciting 10% of the maximum spike number of each non-monotonic spike-stimulus profile.

TABLE I. RGC MORPHOLOGICAL PARAMETERS

RGC	R ( $\mu\text{m}$ )	L ( $\mu\text{m}$ )	S ( $\mu\text{m}$ )
ON	287	7300	10
OFF	218	6700	50

R, radius of dendritic field area, L, total length of dendrites, S, vertical distance between the soma and the dendritic tree layer. All parameters were estimated based on published statistics of ON and OFF RGC morphologies [9].

TABLE II. IONIC CHANNEL DISTRIBUTIONS

Channel	Regional Maximum Membrane Conductances ( $\text{mS}/\text{cm}^2$ )				
	Soma	Axon	AIS	Hillock	Dendrites
ON					
$I_{\text{Na}}$	68.4	68.4	254.1	68.4	7.2
$I_{\text{K}}$	45.9	45.9	68.85	45.9	42.83
$I_{\text{KA}}$	18.9	---	18.9	18.9	13.86
$I_{\text{Ca}}$	1.6	---	1.6	1.6	2.133
$I_{\text{KCa}}$	0.0474	0.0474	0.0474	0.0474	---
$I_{\text{h}}$	0.0286	0.0286	0.0286	0.0286	0.0572
$I_{\text{CaT}}$	---	---	---	---	---
$I_{\text{L}}$	0.2590	0.2590	0.2590	0.2590	0.2590
OFF					
$I_{\text{Na}}$	45.6	45.6	165.9	45.6	4.818
$I_{\text{K}}$	45.9	45.9	68.85	45.9	42.83
$I_{\text{KA}}$	18.9	---	18.9	18.9	13.86
$I_{\text{Ca}}$	1.6	---	1.6	1.6	2.133
$I_{\text{KCa}}$	0.0474	0.0474	0.0474	0.0474	---
$I_{\text{h}}$	2.1	2.1	2.1	2.1	4.2
$I_{\text{CaT}}$	0.1983	0.1983	0.1983	0.1983	0.9915
$I_{\text{L}}$	0.0519	0.0519	0.0519	0.0519	0.0519

$I_{\text{Na}}$ , sodium current,  $I_{\text{K}}$ , delayed rectifier potassium current,  $I_{\text{KA}}$ , type potassium current,  $I_{\text{Ca}}$ , calcium current,  $I_{\text{KCa}}$ , Ca-activated potassium,  $I_{\text{h}}$ , Hyperpolarization activated current,  $I_{\text{CaT}}$ , Low threshold voltage-activated calcium current,  $I_{\text{L}}$ , leakage current.

The preferential activation map in Fig. 1B2 provides an alternative visualisation of differential activation of RGC types at each stimulation frequency and amplitude. Each grid point was determined as the ratio of total spike number (spikes/200 ms) of one cell type over the other. That is,  $\text{ON}/(\text{OFF}+1)$  for ON preferential activation and  $\text{OFF}/(\text{ON}+1)$  for OFF preferential activation. Our model suggested that preferential activation of the ON RGCs was maximized at high stimulation amplitudes ( $> 50 \mu\text{A}$ ) and frequencies (between 2 - 6 kHz). In contrast, HFS pulse trains across all tested frequencies were able to induce robust preferential

activation of OFF RGCs with different stimulation amplitudes ranging from 10 to 50  $\mu\text{A}$ .

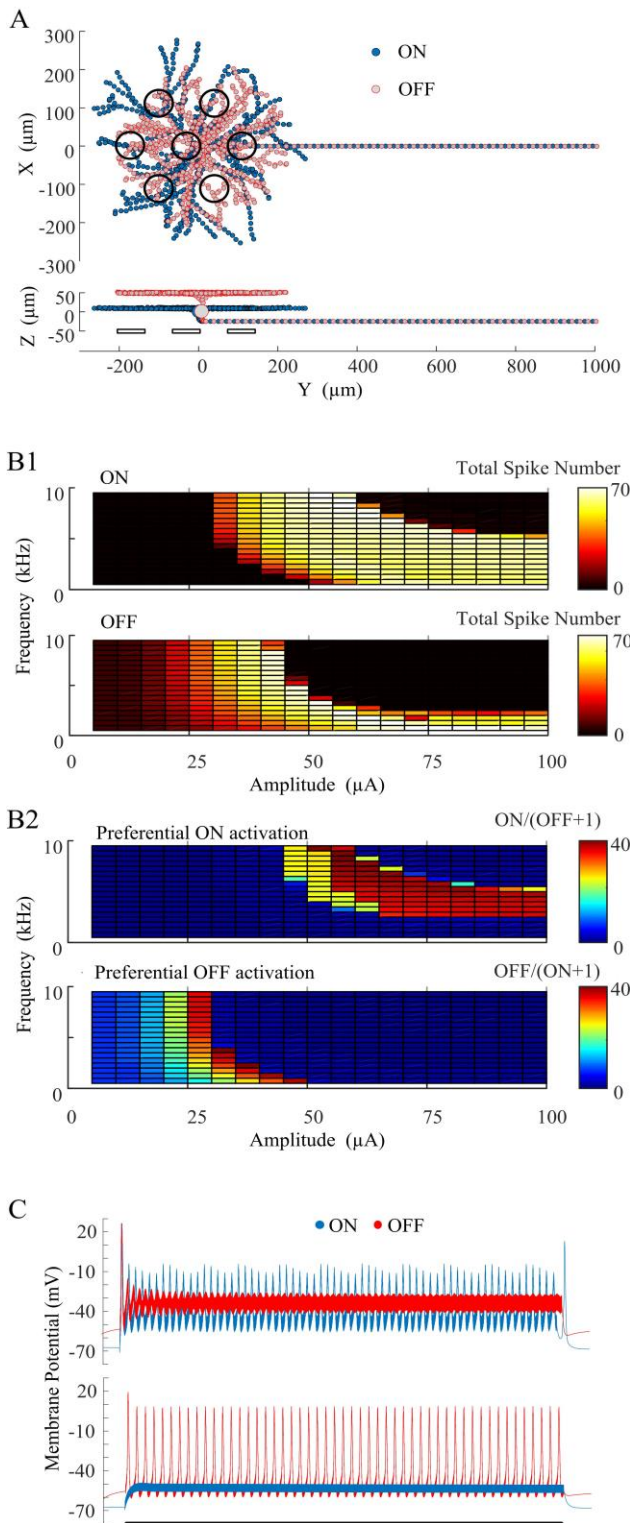


Figure 1. A. Computational models of ON and OFF RGCs with a hexapolar electrode array above the soma. The radius of each disc electrode was  $15\ \mu\text{m}$ , with a center-to-center spacing of  $60\ \mu\text{m}$ . ON and OFF RGC models exhibited significantly different channel densities and morphologies, which contributed to the cell-specific firing patterns in response to HFS. B1. Total spike number (spikes/200 ms) elicited in the model ON and OFF RGCs in

response to a range of stimulation amplitudes (0 - 100  $\mu\text{A}$ ) and frequencies (1 - 10 kHz) delivered over a 200-ms interval. B2: Differential map of RGC excitability represented by the ratio of total spike numbers (spikes/200 ms) for one cell type over the other, indicating stimulation parameters which can preferentially activate one cell type, while minimally activating the other type. C. Upper panel, examples of RGC responses from the ON and OFF RGC models in panel B. With 8-kHz stimuli of  $60\ \mu\text{A}$ , the ON RGC was strongly activated, while simultaneously blocking the OFF RGC spontaneous spikes, yielding only stimulus artifacts. Lower panel, with 7.5-kHz stimuli of  $30\ \mu\text{A}$ , the OFF RGC was strongly activated, whilst the ON RGC remained silent.

Moreover, in Fig.1B2, the threshold at which preferential activation began for both cell types gradually reduced as the stimulus frequency was increased from 1 to 6 kHz. The stimulation current range for preferentially activating ON RGCs increased when the stimulus frequency increased from 2 to 6 kHz, then gradually decreased when the stimulation frequency increased from 6.5 to 10 kHz. In contrast, the stimulation current range for preferentially activating OFF RGCs was mostly stable across all frequencies.

Fig.1C shows examples of preferential RGC recruitment. When the HFS was delivered at 8 kHz and  $60\ \mu\text{A}$ , the ON RGC (blue) was strongly activated, whilst the OFF RGC (red) was blocked. However, when the HFS was delivered at 7.5 kHz and  $30\ \mu\text{A}$ , the OFF RGC was strongly activated, whilst the ON RGC was silenced. These results illustrate promising opportunities for eliciting RGC responses that resemble light-evoked ON/OFF RGC responses, with opposing polarity, through HFS-based electrical stimulation. That is, one RGC type exhibited an increase in spiking activity during HFS while another type exhibited decreased spiking activity given the identical stimulation.

#### IV. DISCUSSION AND CONCLUSION

Computational RGC models provide the ability to investigate neural modulation, by changing key stimulation parameters. One advantage of the computational approach is that the model-generated response space map can be made arbitrarily large and fine-grained, for thorough exploration of stimulus parameters. This is difficult, if not impossible to achieve through biological experiments, due to the invasiveness of intracellular recordings.

Discriminating between ON and OFF RGCs with electrical stimulation is an initial step towards improving artificial vision. Until recently, retinal stimulation has not been able to provide preferential activation of ON and OFF RGCs. Such co-activation is highly unnatural, providing conflicting information to higher visual centers, and potentially degrading the efficacy of retinal implants. In this study, we built on previous *in vitro* [5, 8, 18, 19] and *in silico* [6, 7, 17, 20] studies, demonstrating that preferential activation of individual RGC types can be achieved. Here we further show that the effect is possible over a wide range of HFS parameters. In particular, the ON RGC can be targeted at relatively higher stimulation amplitudes ( $> 50\ \mu\text{A}$ ) and frequencies (2-10 kHz), whilst the OFF RGC can be targeted with lower stimulation amplitudes (10 - 50  $\mu\text{A}$ ), across all tested frequencies (1 - 10 kHz). The precise mechanisms

underlying differential RGC activation remains largely unknown. Further modeling and *in vitro* studies are still required to better understand the factors that shape the response of a retinal neuron to biphasic HFS. In particular, efforts should be devoted to assessing the contribution of intrinsic RGC properties in shaping RGC spiking profiles.

The HFS-based stimulation strategy described here may be useful for more closely mimicking natural encoding of RGC visual patterns. Specifically, the ON ganglion cells showed an increase in spike counts (spikes/200 ms) as the stimulus current was increased, whilst the OFF RGC responses were inhibited by the same stimulus, and vice versa. In addition, our results suggest that preferential activation of the ON RGC may be maximized within the stimulation frequencies 2 ~ 6 kHz, over a wide stimulus current range (50 - 100  $\mu$ A), as shown in Fig.1B2. However, it should be noted that higher frequencies can degrade stimulation efficacy [18, 21]. Therefore, a balance between current amplitude and HFS frequency may be necessary for a practical stimulation strategy. The modelling approach can predict where the optimal stimulation parameters space is likely to be without detailed experimental evaluations, providing insights into stimulation strategies that may benefit from further development.

There are several considerations that may arise when translating these findings to a clinical setting. First, the size and the location of the stimulus electrodes used in existing HFS-based studies are far smaller and closer to the target neurons than those used in clinical devices. Generalizing HFS-based preferential activation from epiretinal stimulation to subretinal and suprachoroidal stimulation placements, over a wide range of electrode sizes, will be an important future work. Second, the combination of a 30  $\mu$ m diameter electrode with 100  $\mu$ A stimulus amplitude used in this study exceeds the reported safe charge injection limits for electrodes fabricated from Pt-black or similar materials [22]. This issue can be mitigated by changing electrode material, increasing electrode size, or changing the stimulus pulse width. Third, we only considered the total number of evoked spikes. In future work, it would be useful to also consider the temporal pattern of the evoked spikes. Finally, our present results are limited to pairs of ON and OFF RGCs: further studies are required to validate the generalizability of preferential activation for a large RGC population.

#### REFERENCES

[1] J. F. Rizzo, J. Wyatt, J. Loewenstein, S. Kelly, and D. Shire, "Perceptual efficacy of electrical stimulation of human retina with a microelectrode array during short-term surgical trials," *Invest Ophthalmol Vis Sci*, vol. 44, pp. 5362-5369, 2003.

[2] E. Zrenner, K. U. Bartz-Schmidt, H. Benav, D. Besch, A. Bruckmann, V. P. Gabel, *et al.*, "Subretinal electronic chips allow blind patients to read letters and combine them to words," *P Roy Soc B-Biol Sci*, vol. 278, pp. 1489-1497, 2011.

[3] M. S. Humayun, J. D. Weiland, G. Y. Fujii, R. Greenberg, R. Williamson, J. Little, *et al.*, "Visual perception in a blind subject with a chronic microelectronic retinal prosthesis," *Vision Res*, vol. 43, pp. 2573-2581, 2003.

[4] N. C. Sinclair, M. N. Shivdasani, T. Perera, L. N. Gillespie, H. J. McDermott, L. N. Ayton, *et al.*, "The appearance of phosphenes elicited using a suprachoroidal retinal prosthesis," *Invest Ophthalmol Vis Sci*, vol. 57, pp. 4948-4961, 2016.

[5] P. Twyford, C. Cai, and S. Fried, "Differential responses to high-frequency electrical stimulation in on and off retinal ganglion cells," *J Neural Eng*, vol. 11, p. 025001, 2014.

[6] T. Kameneva, M. I. Maturana, A. E. Hadjinicolaou, S. L. Cloherty, M. R. Ibbotson, D. B. Grayden, *et al.*, "Retinal ganglion cells: Mechanisms underlying depolarization block and differential responses to high frequency electrical stimulation of on and off cells," *J Neural Eng*, vol. 13, p. 016017, 2016.

[7] T. Guo, N. H. Lovell, D. Tsai, P. Twyford, S. Fried, J. W. Morley, *et al.*, "Selective activation of on and off retinal ganglion cells to high-frequency electrical stimulation: A modeling study," presented at the 36th Annual International Conference of the IEEE Engineering in Medicine and Biology Society, Chicago, US, 2014.

[8] C. Cai, P. Twyford, and S. Fried, "The response of retinal neurons to high-frequency stimulation," *J Neural Eng*, vol. 10, p. 036009, 2013.

[9] C. P. Ratliff, B. G. Borghuis, Y. H. Kao, P. Sterling, and V. Balasubramanian, "Retina is structured to process an excess of darkness in natural scenes," *P Natl Acad Sci USA*, vol. 107, pp. 17368-17373, 2010.

[10] M. L. Hines and N. T. Carnevale, "The neuron simulation environment," *Neural Computation*, vol. 9, pp. 1179-209, 1997.

[11] T. Guo, D. Tsai, J. W. Morley, G. J. Suaning, T. Kameneva, N. H. Lovell, *et al.*, "Electrical activity of on and off retinal ganglion cells: A modelling study," *J Neural Eng*, vol. 13, p. 025005, 2016.

[12] S. W. Bai, T. R. Guo, D. Tsai, J. W. Morley, G. J. Suaning, N. H. Lovell, *et al.*, "Influence of retinal ganglion cell morphology on neuronal response properties - a simulation study," presented at the 2015 7th International IEEE/EMBS Conference on Neural Engineering, Paris, France, 2015.

[13] H. Cuntz, F. Forstner, A. Borst, and M. Hausser, "One rule to grow them all: A general theory of neuronal branching and its practical application," *PLoS Comput Biol*, vol. 6, 2010.

[14] R. C. Prim, "Shortest connection networks and some generalizations," *At&T Tech J*, vol. 36, pp. 1389-1401, 1957.

[15] D. Tsai, S. Chen, D. A. Protti, J. W. Morley, G. J. Suaning, and N. H. Lovell, "Responses of retinal ganglion cells to extracellular electrical stimulation, from single cell to population: Model-based analysis," *PLoS One*, vol. 7, p. e53357, 2012.

[16] J. K. Mueller and W. M. Grill, "Model-based analysis of multiple electrode array stimulation for epiretinal visual prostheses," *J Neural Eng*, vol. 10, 2013.

[17] T. Guo, N. H. Lovell, D. Tsai, P. Twyford, S. Fried, J. W. Morley, *et al.*, "Optimizing retinal ganglion cell responses to high-frequency electrical stimulation strategies for preferential neuronal excitation," presented at the 2015 7th International IEEE/EMBS Conference on Neural Engineering, Paris, France, 2015.

[18] C. S. Cai, Q. S. Ren, N. J. Desai, J. F. Rizzo, and S. I. Fried, "Response variability to high rates of electric stimulation in retinal ganglion cells," *J Neurophysiol*, vol. 106, pp. 153-162, 2011.

[19] T. Guo, C. Y. Yang, D. Tsai, M. Muralidharan, G. J. Suaning, J. W. Morley, *et al.*, "Closed-loop efficient searching of optimal electrical stimulation parameters for preferential excitation of retinal ganglion cells," *Front Neurosci*, vol. 12, 2018.

[20] T. Guo, A. Barriga-Rivera, G. J. Suaning, D. Tsai, S. Dokos, J. W. Morley, *et al.*, "Mimicking natural neural encoding through retinal electrostimulation," presented at the 2017 8th International International IEEE/EMBS Conference on Neural Engineering, Shanghai, China, 2017.

[21] A. E. Hadjinicolaou, C. O. Savage, N. V. Apollo, D. J. Garrett, S. L. Cloherty, M. R. Ibbotson, *et al.*, "Optimizing the electrical stimulation of retinal ganglion cells," *IEEE Trans Neur Sys Reh*, vol. 23, pp. 169-178, 2015.

[22] T. L. Rose and L. S. Robblee, "Electrical stimulation with pt electrodes. Viii. Electrochemically safe charge injection limits with 0.2 ms pulses," *IEEE Trans Biomed Eng*, vol. 37, pp. 1118-20, 1990.